ELSEVIER

Journal of Nuclear Materials 317 (2003) 69–82

journal of nuclear materials

www.elsevier.com/locate/jnucmat

Statistical approach and benchmarking for modeling of multi-dimensional behavior in TRISO-coated fuel particles

Gregory K. Miller *, David A. Petti, Dominic J. Varacalle Jr., John T. Maki

Idaho National Engineering and Environmental Laboratory, P.O. Box 1625, Idaho Falls, ID 83415-3765, USA

Received 10 October 2002; accepted 10 December 2002

Abstract

The fundamental design for a gas-cooled reactor relies on the behavior of the coated particle fuel. The coating layers, termed the TRISO coating, act as a mini-pressure vessel that retains fission products. Results of US irradiation experiments show that many more fuel particles have failed than can be attributed to one-dimensional pressure vessel failures alone. Post-irradiation examinations indicate that multi-dimensional effects, such as the presence of irradiation-induced shrinkage cracks in the inner pyrolytic carbon layer, contribute to these failures. To address these effects, the methods of prior one-dimensional models are expanded to capture the stress intensification associated with multi-dimensional behavior. An approximation of the stress levels enables the treatment of statistical variations in numerous design parameters and Monte Carlo sampling over a large number of particles. The approach is shown to make reasonable predictions when used to calculate failure probabilities for irradiation experiments of the New Production – Modular High Temperature Gas Cooled Reactor Program.

1. Introduction

The success of gas-cooled reactors depends largely upon the safety and quality of the coated particle fuel. The coating layers of a particle, which surround the fuel kernel and buffer, consist of an inner pyrolytic carbon (IPyC) layer, a silicon carbide (SiC) layer, and an outer pyrocarbon (OPyC) layer. These layers act as a pressure vessel for fission product gases as well as a barrier to the migration of other fission products. The quality of the fuel can be characterized by how well the number of failures of the particles during reactor operation is minimized. Therefore, a performance model of the coating layers is needed to determine the failure probability of a population of fuel particles. Such a model must account for all viable mechanisms that can lead to particle failure.

Early models of coated fuel particles such as that of Kaae [1] used iterative numerical procedures to include the effects of pyrocarbon creep and swelling in determining stresses in the coating layers. Stevens' closed form solution for a single layer [2] significantly increased the speed for calculating stresses, making it possible to perform Monte Carlo investigations of particle behavior. Gulden et al [3] studied the effects of assuming a Gaussian distribution for kernel diameter and buffer thickness on particle failures, and Bongartz [4] added the effect of a Weibull distribution for SiC strengths. Bongartz used the Walther model [5] to perform his calculations, a comprehensive model developed during the Dragon project that is formulated in terms of linearized increments. Bongartz [6] simplified the stress analysis with a closed form solution based on the assumption of a rigid SiC layer, which enhanced the speed of Monte Carlo calculations. Miller and Bennett [7] derived a closed form solution for a three-layer particle, allowing for a flexible SiC layer. All of these are one-dimensional models (benefiting from spherical symmetry) used to evaluate a pressure vessel failure of the coating layers.

* Corresponding author. Tel.: +1-208 526 0360; fax: +1-208 526 4313.

E-mail address: gkm@inel.gov (G.K. Miller).

0022-3115/03/$ - see front matter
doi:10.1016/S0022-3115(02)01702-6

Nomenclature

$f(\Delta v)$	function that describes the variation of maximum stress in the SiC layer of a cracked particle with parameter v
$g(\Delta v)$	function that describes the variation of maximum stress in the SiC layer of an uncracked particle with parameter v
$h(\Delta v)$	ratio $f(\Delta v)/g(\Delta)$
I	normalized integration of the stress distribution over the volume of the SiC layer (μm^3)
m	Weibull modulus for SiC
P_f	probability of failure for the SiC
V	volume of the SiC layer (μm^3)
σ	stress in the SiC layer (MPa)
σ_c	stress in the SiC layer for a particle having a cracked IPyC (MPa)
σ_s	strength for the SiC layer in a random particle as sampled from a Weibull distribution (MPa)
σ_u	stress in the SiC layer for an uncracked particle (MPa)
$\sigma_{c\bar{v}}$	stress in the SiC layer for a cracked particle having all parameters set at mean values for a particle batch (MPa)
$\sigma_{u\bar{v}}$	stress in the SiC layer for an uncracked particle having all parameters set at mean values for a particle batch (MPa)
σ_0	Weibull characteristic strength for the SiC layer (MPa $\mu m^{3/m}$)
σ_{ms}	effective mean strength for the SiC layer in particles having a cracked IPyC (MPa)
σ_i	$i = 1, 2, 3$, principal stress components in three orthogonal directions (MPa)
Δv	variation in parameter v from its mean value

The STRESS3 Code is based on Walther's model, and is the result of developments by Bongartz and Martin [8]. With its incremental solution, it is flexible in allowing for the analysis of up to six layers and in allowing material properties in the layers to change as irradiation progresses. When used in conjunction with the STAPLE Code, it performs Monte Carlo calculations that incorporate statistical variations in design parameters and Weibull distributions in the strength of the coating layers. Its model is also one dimensional, but it addresses particle failures caused by mechanical interaction between the fuel kernel and the coating layers in addition to the traditional pressure vessel failure.

The fuel of the New Production – Modular High Temperature Gas Cooled Reactor (NP-MHTGR) as well as other coated fuel designed in the US has incurred significantly greater levels of failure than are predicted considering just pressure vessel failures, indicating that other mechanisms contributed to failure of the particles. Post-irradiation examination (PIE) revealed the presence of radial shrinkage cracks in the IPyC and OPyC layers, and partial debonding between the IPyC and the SiC. It was recently shown that shrinkage cracks in the IPyC layer can contribute significantly to the failure of fuel particles [9]. Therefore, multi-dimensional effects may well have led to the unexpectedly large number of failures of fuel particles in the US.

To aid in investigating such coated particle fuels, the Idaho National Engineering and Environmental Laboratory (INEEL) is developing an integrated mechanistic fuel performance model called PARticle FUel ModEl (PARFUME). An objective is to represent the multi-dimensional behavior associated with anomalies such as shrinkage cracking, partial debonding, and asphericity. The methodology described herein and incorporated in the PARFUME Code adds the effect of the stress intensification associated with a cracked IPyC to previous fuel performance models. It utilizes the results of detailed finite element analysis on a cracked particle (using the ABAQUS program [10]) to make a statistical approximation of the stress levels in a particle. As with previous models, the method incorporates a Weibull distribution in strengths for the coating layers. Numerous parameters can be varied statistically using the approximation including thicknesses of the three coating layers, densities of the pyrocarbons, degree of anisotropy in the pyrocarbons, irradiation temperature, the creep coefficient for the pyrocarbons, kernel diameter, buffer thickness, and Poisson's ratio in creep for the pyrocarbons. The statistical approximation is used in Monte Carlo sampling in PARFUME to efficiently estimate stresses in a set of random particles, and thereby calculate failure probabilities. The method is described herein in terms of particles having a cracked IPyC layer, but is in principle applicable to other multi-dimensional mechanisms.

Results obtained are compared to results from a sixth-order polynomial algorithm that was developed from regression analysis of multi-dimensional finite element analysis results. The model is then used to predict failure probabilities for irradiation experiments of the NP-MHTGR program.

2. Mechanical modeling of gas reactor fuel

The method presented herein requires performing finite element stress analyses on TRISO-coated fuel particles to characterize the multi-dimensional behavior of the fuel particle. A finite element model using the ABAQUS program for a cracked three-layer geometry is shown in Fig. 1. The model, which is axisymmetric to capture the effect of a full sphere, incorporates the behavior shown in Fig. 2. Fission gas pressure builds up in the kernel and buffer regions, while the IPyC, SiC, and OPyC act as structural layers to retain this pressure. The IPyC and OPyC layers both shrink and creep during irradiation of the particle while the SiC exhibits only elastic response. A portion of the gas pressure is transmitted through the IPyC layer to the SiC. This pressure continually increases as irradiation of the particle progresses, thereby contributing to a tensile hoop stress in the SiC layer. Countering the effect of the pressure load is the shrinkage of the IPyC and OPyC layers during irradiation, which causes them to push or pull inward on the SiC. Due to anisotropy in the pyrocarbon shrinkage behavior, the shrinkage histories differ for the radial and tangential directions. The shrinkage in the radial direction reverses to swelling at moderate fluence levels, whereas shrinkage in the tangential direction continues to high fluence levels.

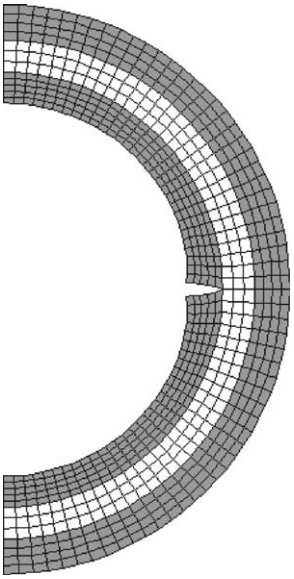

Fig. 1. Finite element model for fuel particle having radial crack in IPyC layer.

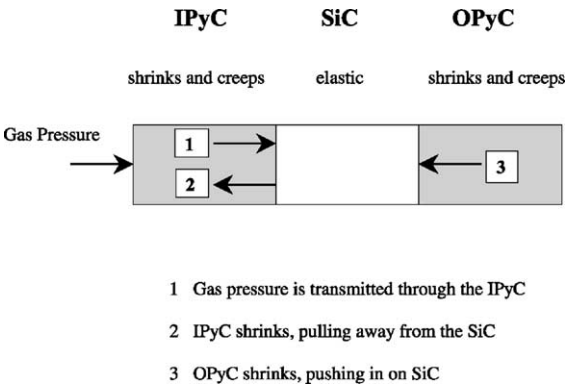

Fig. 2. Behavior of coating layers in fuel particle.

The crack in the IPyC is typical of those observed in PIE of the NP-MHTGR fuel particles. During irradiation, shrinkage of the initially intact IPyC layer induces a significant tensile stress in that layer. If the stress exceeds the tensile strength of the IPyC layer, then a radial crack develops in the IPyC. This crack is included in the model from the beginning of the ABAQUS solution, since it is not feasible to initiate the crack later in the analysis. Because the shrinkage in the pyrocarbons dominates the particle behavior early during irradiation, large tensile stresses in the IPyC occur early. Therefore, the assumption of the presence of a crack from the beginning of the solution should be a reasonable approximation. The analysis does not include any dynamic effects associated with a sudden failure of the IPyC, which could increase the magnitude of the stresses calculated. Potential cracks in the OPyC layer are not addressed here because, at the lower stress levels in the OPyC, these are much less likely to contribute to SiC failures.

In the finite element analyses performed, an internal pressure is applied to simulate the fission gas build-up. The shrinkage strain rates and creep coefficients for the pyrocarbons and the elastic properties for the pyrocarbons and the SiC were obtained from data that was compiled in a report by General Atomics in 1993 [11]. As such, the shrinkage strains are treated as functions of four variables, i.e., fluence level, pyrocarbon density, degree of anisotropy (as measured by the Bacon Anisotropy Factor (BAF)), and irradiation temperature. Irradiation-induced creep is treated as secondary creep, with a coefficient that is a function of pyrocarbon density and irradiation temperature. The elastic modulus for the pyrocarbon layers is applied as a function of four variables (the same variables as used for shrinkage), while the elastic modulus for SiC is applied as a function of temperature only. As discussed in [8], there is some doubt as to how well these physical properties of the coating layers are known, which becomes especially important when fuel particles are required to attain high burnups.

Particles discussed herein are analyzed in a viscoelastic time-integration analysis that progresses until the

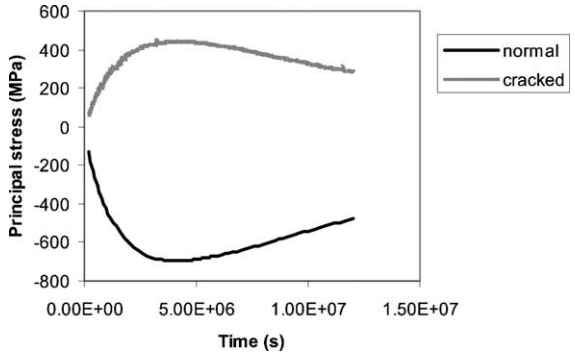

Fig. 3. SiC stress histories for normal and cracked particles.

fluence reaches a specified value (typically 3×10^{25} n/m^2, occurring at a time of 1.2×10^7 s in the analysis). Fig. 3 plots a time evolution for the tangential stress at the inner surface of the SiC layer for a particle having no crack in the IPyC. Early during irradiation, the shrinkage of the pyrocarbon layers induces an increasing compressive stress in the SiC. Eventually, creep in the pyrocarbon layers relieves stress in those layers, diminishing the beneficial effect of the shrinkage. Therefore, the tangential stress in the SiC reaches a minimum value then steadily increases through the remainder of irradiation. Fig. 3 also plots a time history for the maximum calculated principal stress in the SiC layer of a particle having a cracked IPyC. This stress was calculated at an integration point near the crack tip, since it is not feasible to accurately calculate stresses right at the tip. The maximum stress in the vicinity of the crack tip quickly becomes tensile, rising to a peak value at a time of 0.4×10^7 s. Again, creep in the pyrocarbon layers relieves stress in those layers, and the SiC stress around the crack tip falls off. The stress histories for the two particles are similar in reaching maximum magnitudes at the same time during irradiation.

3. Parametric analysis

3.1. Effects analysis

Variations in the twelve parameters listed in Table 1 are expected to affect the stress levels in a fuel particle to varying degrees. Stress analyses using ABAQUS were performed to determine the effect that each of these parameters has on the stress level in the SiC layer of a particle having a cracked IPyC layer. First, nominal values were identified for each of the parameters (as shown in the table), which are intended to be representative of the particle design for gas-cooled reactors. Then, analyses were performed in which the parameters were varied over the ranges shown. In each analysis performed, a single parameter was varied from its nominal value and was held constant at that value throughout the analysis. Because the algorithm for creep behavior in the ABAQUS program allows only a value of 0.5 for Poisson's ratio, the effects for this parameter were based on analyses of an uncracked particle in the PARFUME code. In all cases analyzed, the same value was used for Poisson's ratio in creep for both pyrocarbon layers. The large range of kernel diameters covers the smaller diameters of high-enriched kernels to the larger diameters of low-enriched kernels. Particles for gas reactors are expected to be on the order of 500 μm. The wide range in the creep coefficient addresses the considerable uncertainty in values reported in the literature for this property.

Table 1
Results of effects analysis for parametric variations

Parameter	Nominal value	Range of variation	Influence factor
IPyC BAF	1.06	1.0–1.18	3.83
OPyC BAF	1.06	1.0–1.18	2.09
IPyC thickness (μm)	40	30–50	1.66
Creep (10^{29} MPa-n/m^2)$^{-1}$	2.71	1.36–4.75	1.55
SiC thickness (μm)	35	25–45	1.51
IPyC density (10^6 g/m^3)	1.9	1.8–2	1.20
Irradiation temperature (°C)	1000	600–1250	1.0
Poisson's ratio in creep	0.5	0.3–0.5	0.86
Kernel diameter (μm)	500	175–650	0.75
OPyC density (10^6 g/m^3)	1.9	1.8–2	0.71
OPyC thickness (μm)	40	30–50	0.55
Buffer thickness (μm)	100	80–120	0.19

Results of the analyses are reported in terms of an influence factor, which is the percent change in maximum SiC stress divided by the percent variation in that parameter (from its nominal value). An influence factor was calculated for each parameter at the two extremes of the range of variation shown in the table. The larger of these two values was then selected as the measure of degree of influence for that parameter. The parameters are arranged in the table according to the degree of influence, indicating that the BAFs of the pyrocarbon layers are the most influential parameters. It is noted that the influence factors are dependent upon what are selected as nominal values for the parameters.

Results of the effects analysis for four key parameters (i.e., IPyC BAF, irradiation temperature, creep amplification, and kernel diameter) are shown graphically in Fig. 4. An increasing BAF increases the shrinkage in the IPyC layer, which increases stresses in the particle layers. Increasing creep in the pyrocarbons tends to relax the shrinkage stresses, therefore resulting in decreasing stresses in the layers. An increasing irradiation temperature increases both the shrinkage and creep in the py-

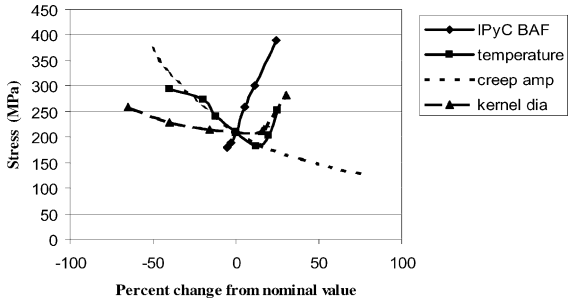

Fig. 4. Effect of variations in key parameters on the SiC stress in a cracked particle.

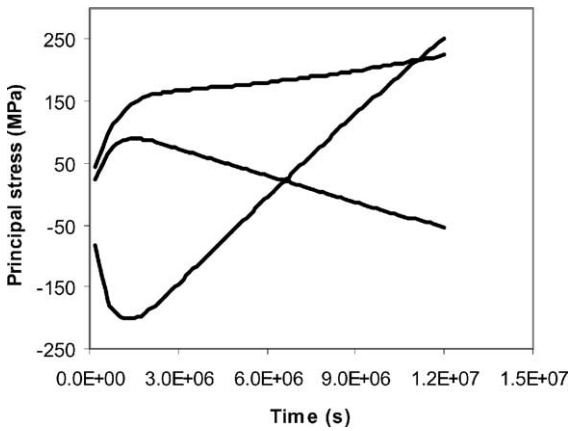

Fig. 5. Three components of principal stress in SiC layer of cracked particle at irradiation temperature of 1250 °C.

rocarbons. Up to a temperature of about 1200 °C, the higher creep more than offsets the shrinkage effect, resulting in lower SiC stresses. At higher temperatures, though, the creep fails to reverse the stresses, and the maximum principal stress increases steadily until the end of irradiation (see Fig. 5). Fig. 5 also shows that an initially compressive stress component reaches a significant tensile value by the end of irradiation. Depending on when irradiation ends, this stress may be the largest that occurs in the stress history. An increasing kernel diameter tends to decrease the maximum stress in the SiC layer for diameters up to about 500 μm. At larger diameters, an initially compressive stress component reaches a significant tensile value by the end of irradiation. As with a high-temperature calculation, the maximum stress may not be reached until the end of irradiation.

3.2. Algorithm based on response surface methodology

In addressing multi-dimensional behavior in fuel particles, statistical analysis is used to develop equations that can efficiently calculate stresses in a random particle, where several parameters may deviate from their mean. These equations are used in turn in a Monte Carlo simulation to calculate failure probabilities for a batch of fuel particles. Initially, the Design Expert program [12] was used to perform a regression analysis to produce an algorithm that predicts the stress level in the SiC layer of particles that have a cracked IPyC layer. This program uses Box response surface analysis [13] to develop a polynomial that statistically fits stress data to a high level of accuracy when variations in several parameters are considered. A response surface defines the response of an analytical experiment to variations in multiple factors. In this initial work, statistical variations were performed on six parameters that affect behavior of a fuel particle. These parameters and the values at which each was analyzed are listed in Table 2. Nominal values listed are simply midpoints for the range whereas those in Table 1 are more representative of actual fuel production attributes. A three-level full-factorial regression analysis was performed for four irradiation temperatures, which required 972 finite element analysis runs to analyze all possible combinations of the values listed in the table. A variance analysis using Design Expert indicated that a sixth-order polynomial was needed to sufficiently fit the data. The program was thus used to produce a sixth-order polynomial algorithm, whereby the stresses calculated with the algorithm matched the ABAQUS stresses (for the 972 cases) to within 0.5% accuracy. The algorithm was incorporated in the fuel performance model as a method of calculating maximum SiC stresses in cracked particles.

The Design Expert methodology is a powerful statistical tool that successfully produced a fast running algorithm that calculates stresses for variations in the parameters listed in Table 2. Its capacity for these purposes, though, is essentially reached with variations in six parameters when a full-factorial analysis is desired. Introducing more parameters would likely require a yet higher-order polynomial to attain sufficient accuracy, which is not achievable in the program. Furthermore, a full-factorial regression analysis over more parameters

Table 2
Parametric values used in Design Expert analyses

Parameter	Values for finite element analyses	Nominal value
IPyC thickness (μm)	30, 40, 50	40
SiC thickness (μm)	25, 35, 45	35
OPyC thickness (μm)	33, 43, 53	43
IPyC density (10^6 g/m^3)	1.8, 1.9, 2.0	1.9
IPyC BAF	1.0, 1.16, 1.32	1.16
Irradiation temperature (°C)	600, 800, 1000, 1200	1000

would require a prohibitive number of finite element analyses. Even if only six parameters are considered, a change in fundamental assumptions going into the statistical analysis may require rerunning all of the finite element analyses to develop a new algorithm. An alternative means has been developed for approximating the multi-dimensional stresses for the SiC to accommodate statistical variations in a large number of parameters and to enable treatment of new multi-dimensional failure mechanisms. Particle failure probabilities calculated using this new approach have been benchmarked against results obtained from the Design Expert algorithm.

4. New statistical approximation for SiC stress

The approximation described below greatly reduces the number of finite element analyses needed and allows for variations in any number of parameters. It somewhat follows the approach given in [14] for treating asphericity in fuel particles, but is more generally applicable to other multi-dimensional mechanisms. In this approach, finite element analyses are performed on just enough cases to determine the effects of varying each parameter individually. The same cases are then analyzed using a closed-form solution that solves for stresses in a normal (uncracked) TRISO fuel particle [7]. Finally, statistical fits are performed on the results of the analyses and a correlation is drawn between the stress in an uncracked particle with the stress in a cracked particle for the same parametric variations.

4.1. Parametric variations about mean values

The statistical approach is developed in terms of variations about mean values for the parameters that describe a batch of fuel particles. A set of mean values for any particular batch of particles is generally unique to that batch, differing from those listed in Tables 1 or 2. Therefore, the method must be flexible in addressing any set of mean values. When all parameters in a cracked particle are at their mean values, the maximum calculated stress in the SiC layer of the particle assumes a value $\sigma_{c\bar{v}}$. If a single parameter v varies from its mean value by an amount Δv, then a function $f(\Delta v)$ can be introduced such that the stress can be expressed in terms of $\sigma_{c\bar{v}}$ as follows:

$$\sigma_c(v) = \sigma_{c\bar{v}} f(\Delta v). \tag{1}$$

Likewise, a function $g(\Delta v)$ can be introduced such that the maximum stress in an uncracked particle can be expressed as follows (for the same parametric variation):

$$\sigma_u(v) = \sigma_{u\bar{v}} g(\Delta v). \tag{2}$$

The stress for the cracked particle $\sigma_{c\bar{v}}$ is determined from a finite element analysis, while the stress for an uncracked particle $\sigma_{u\bar{v}}$ is determined readily from the closed-form solution in the performance model. The functions f and g can generally be expressed as follows:

$$f(\Delta v) = e^{a_1 \Delta v + a_2 \Delta v^2}, \tag{3}$$

$$g(\Delta v) = e^{b_1 \Delta v + b_2 \Delta v^2}. \tag{4}$$

Dividing Eq. (1) by Eq. (2) results in the following equation:

$$\sigma_c(v) = \frac{\sigma_{c\bar{v}}}{\sigma_{u\bar{v}}} \sigma_u(v) h(\Delta v), \tag{5}$$

where the function h (which is the ratio f/g) will normally fit the following quadratic form (as shown below):

$$h(\Delta v) = 1 + c_1 \Delta v + c_2 \Delta v^2. \tag{6}$$

This is effectively a Taylor series expansion, where all terms above second-order drop out because higher order derivatives become very small. The function h brings the stress in an uncracked particle into correlation with the stress in a cracked particle for any variation in the parameter v. The function h_i would equal 1.0 over the range of Δv_i if the solutions for σ_c and σ_u treated the parametric variations proportionately (i.e., $f(\Delta v_i) = g(\Delta v_i)$). As shown in Fig. 6, which plots h_i for each of the three coating layer thicknesses for the particles described in Table 1, there is normally some deviation from 1.0 when $\Delta v \neq 0$.

When several parameters are varied from their mean values, Eq. (5) for SiC stress in the cracked particle can be expanded as follows:

$$\sigma_c(v_j, v_k, v_l, \ldots) = \frac{\sigma_{c\bar{v}}}{\sigma_{u\bar{v}}} \sigma_u(v_j, v_k, v_l, \ldots) h(\Delta v_j, \Delta v_k, \Delta v_l \ldots). \tag{7}$$

The function h in this equation is a correlation function that approaches 1.0 as the $\Delta v's$ approach zero.

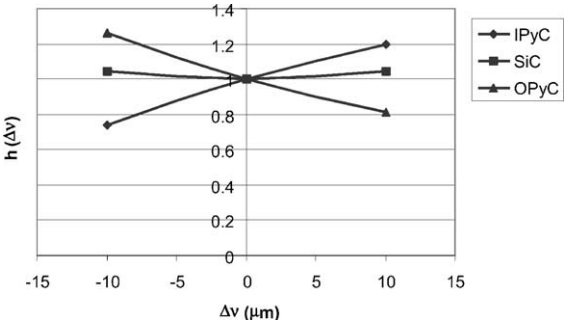

Fig. 6. Functions $h(\Delta v)$ for variations in IPyC, SiC, and OPyC thicknesses.

Provided that the $\Delta v's$ do not become too large, h can be approximated by the product of the individual h_i's, resulting in the following:

$$\sigma_c(v_j, v_k, v_l) \cong \frac{\sigma_{c\bar{v}}}{\sigma_{u\bar{v}}}\sigma_u(v_j, v_k, v_l, \ldots)h_j(\Delta v_j)h_k(\Delta v_k)h_l(\Delta v_l)\ldots \tag{8}$$

The accuracy of using this equation to estimate stresses in the SiC layer for particles in a batch is tested in benchmarking calculations described in Section 6. When used in calculating the failure probability for a batch of particles, functions h_i are needed only for those parameters that vary about a mean value. For parameters having no variation, $\Delta v_i = 0$ and $h_i = 1$. In the limiting case where there are no variations (i.e., no measured variability) in any of the parameters among particles in a batch, the stress in Eq. (8) correctly reduces to the stress $\sigma_{c\bar{v}}$. As explained in Section 6, this results in a theoretically exact failure probability for this situation.

Fig. 7 demonstrates that an h function for a parameter can typically be produced from three data points. This figure plots the h function for IPyC density of the particles in Table 1, ranging 0.1×10^6 g/m^3 to each side of the mean value for this parameter. Since this exceeds four times the expected standard deviation for the pyrocarbon density, this range should encompass all fuel particles in a batch. It is evident that a quadratic fit is optimal for the five points shown, which were obtained from ABAQUS finite element analysis results. The figure actually plots two least-squares fitted curves, i.e. one based on all five points and the other based on three points (the outer two points and midpoint). Since the two curves essentially coincide, the use of three points to generate this curve is sufficient. This was the case for all h functions developed in analyses described herein, when the functions ranged over four standard deviations of a practical magnitude. Therefore, Eq. (8) can be developed from a limited number of finite element analyses, and any number of parameters can be considered. A finite element analysis must first be performed to calculate $\sigma_{c\bar{v}}$, by setting all parameters equal to their respective mean values. This result serves as a midpoint for each of the parameters considered. Determining the function h for a particular parameter then requires that two more finite element analyses be performed, in which that parameter is varied approximately four standard deviations to each side of its mean value. In these analyses, all other parameters are held at their mean values. Results from these two analyses together with the midpoint give three data points for the function f (which is the numerator of h). The same cases are solved for an uncracked particle using the analytical solution in the performance model to produce three corresponding values for the denominator g. A polynomial curve fit is then made on the three resulting values of f/g (the midpoint equals 1.0) to generate the function h.

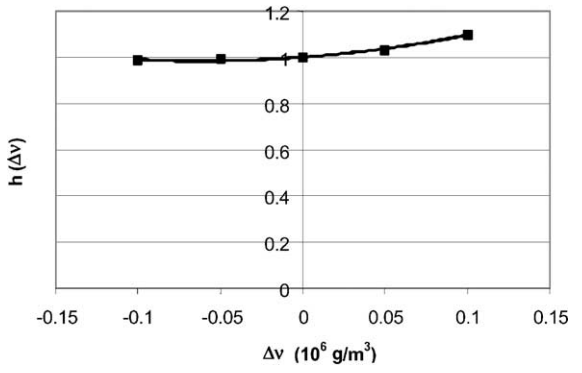

Fig. 7. Generating an h function for variations in IPyC density.

4.2. Simplifying approximation

The correlation functions h_i above are developed by taking variations in the parameters v_i about a set of mean values for a specific batch of fuel particles. Using an Eq. (8) developed for one batch of particles to estimate SiC stresses for another batch of particles (having different mean values) can lead to inaccuracy in the calculated failure probability for the latter. This suggests that a new Eq. (8) should be developed for each batch of fuel particles considered. Doing so would require performing a number of finite element analyses to develop a set of h functions, which may be more work than desired for calculating the failure probability for each batch of particles. To simplify matters, it has been found that a reasonable estimate of the failure probability for a typical batch of particles can be obtained by simply setting the correlation functions equal to one. With this approximation, the SiC stress in the cracked particle is written as follows:

$$\sigma_c(v_j, v_k, v_l, \ldots) \cong \frac{\sigma_{c\bar{v}}}{\sigma_{u\bar{v}}}\sigma_u(v_j, v_k, v_l, \ldots). \tag{9}$$

Eq. (9) requires that only one finite element analysis be performed, i.e. to determine $\sigma_{c\bar{v}}$. It requires no statistical analysis of finite element analysis results. The principle behind Eq. (9) is that, in the random sampling process over many particles, the product of the h functions fluctuates about an average value very near to 1.0. The correlation functions h are greater than 1.0 for some parameters and less than 1.0 for others, and the distribution of these functions on the plus and minus side of 1.0 varies from particle to particle. Furthermore, the average value of $h_i(\Delta_i)$ over a Gaussian distribution for parameter v_i is typically within 1% of 1.0. Therefore, replacing the product of the h functions with a value of 1.0 for all particles in a batch should result in a

reasonable estimate for the failure probability. As with Eq. (8), the stress in Eq. (9) correctly reduces to the stress $\sigma_{c\bar{v}}$ when there are no statistical variations in any of the parameters. The accuracy of using Eq. (9) in calculating batch failure probabilities is tested in benchmarking calculations described in Section 6. The possibility of improving the accuracy of Eq. (9) by selectively including some of the functions h_i from Eq. (8) is explored in Section 7.

5. Determining failure of the SiC

The next step is to utilize the stresses calculated to determine particle failure probabilities in the fuel performance model. Using a fracture mechanics approach to determine whether a cracked IPyC layer results in failure of the SiC is complicated by the fact that there is a material discontinuity at the interface between the IPyC and SiC layers. A crack through the thickness of the IPyC layer does not necessarily induce a flaw in the SiC material. It does, however, create stress concentrations in the SiC material in the vicinity of the crack tip that could lead to particle failure. The SiC failures should follow a Weibull statistical distribution, having a mean strength σ_{ms} and a modulus m. Thus, as with previous models, Weibull statistics is used to evaluate failure of the SiC layer. The mean strength is determined from the characteristic strength σ_0 obtained from data of [11]. In the Weibull theory, the failure probability for the SiC is as follows [15]:

$$P_f = 1 - e^{-\int_V (\sigma/\sigma_0)^m \, dV}. \tag{10}$$

Once finite element results are obtained from the analysis of a cracked particle, the stress integration above can be performed using the principle of independent action model for treating multiaxial stress states [15]:

$$\int_V \sigma^m \, dV = \int_V (\sigma_1^m + \sigma_2^m + \sigma_3^m) \, dV. \tag{11}$$

Since only tensile stresses contribute to fracture of the material, compressive stresses are not included in the integration. Only stresses in the finite elements of the SiC layer in the immediate vicinity of the crack tip make a meaningful contribution to the integral. The integration is performed using stress values calculated at integration points in the ABAQUS analysis.

Based on the magnitude of stresses calculated at integration points near the crack tip, the integral above assumes a value that can be written as follows:

$$\int_V \sigma^m \, dV = \sigma_c^m \int_V f(V) \, dV = \sigma_c^m(I). \tag{12}$$

where σ_c is the maximum value calculated for the stress anywhere in the volume. The integral I is a normalized integration of the stress distribution, where the maximum stress (taken to the m power) has been factored out. The failure probability then becomes

$$P_f = 1 - e^{-\sigma_c^m(I)/\sigma_0^m}. \tag{13}$$

In the fuel performance model, the strength of the SiC layer is sampled according to the following cumulative distribution function [16]:

$$P_f = 1 - e^{-(\sigma_c/\sigma_{ms})^m}. \tag{14}$$

The mean strength σ_{ms} then is determined by applying the condition that the failure probability calculated by the fuel performance model per Eq. (14) equals that of Eq. (13). This is done by equating the exponents of the two equations and using stresses obtained from a finite element analysis on a particle having nominal values for all parameters to determine the integral I. The effective mean strength for the SiC layer of a particle having a cracked IPyC is then defined to be:

$$\sigma_{ms} = \sigma_0 / I_n^{1/m}. \tag{15}$$

where the subscript n denotes a particle having nominal values for all parameters. In the data compiled by CEGA [11], values recommended for the Weibull parameters of the SiC are $m = 6$ and $\sigma_0 = 9640$ MPa $\mu m^{3/6}$. A stress analysis giving $\sigma_{cn} = 441$ MPa and $I_n = 1.58 \times 10^{21}$ μm^3 resulted in an effective mean strength σ_{ms} of 1250 MPa.

Because of the similarity in stress histories for cracked and uncracked particles as exhibited in Fig. 3, Eqs. (8) or (9) can also be used to estimate the time at which failure of the SiC occurs. This is done in a PARFUME analysis by stepping the analytical solution for σ_u forward in time until the stress σ_c, per Eqs. (8) or (9), either reaches a failure stress or its maximum value.

6. Benchmarking of statistical method

6.1. New method (using correlation functions) vs. the Design Expert algorithm

The statistical method described above was tested analytically by using the equations of the method and the algorithm produced by the Design Expert program (Section 3.2) to independently estimate stresses in cracked fuel particles. The stresses from the two methods were used in a Monte Carlo simulation to calculate failure probabilities for fuel particles. The method was then verified by comparing failure probabilities calculated by the two methods.

The fuel particles selected for such a comparison exhibit statistical variations in the six parameters listed in Table 2. The mean values for these six parameters were assumed to match the nominal values of the table. Because the regression analyses of Design Expert were centered on the nominal values of Table 2 (i.e., these nominal values were used as "reference points" in the analysis), results from the Design Expert algorithm for these fuel particles provide a benchmark for measuring accuracy of the new statistical method. Other parameters for the selected particles were assumed to have fixed values for all particles as follows: kernel diameter of 195 μm, buffer thickness of 100 μm, outer pyrocarbon BAF of 1.16, outer pyrocarbon density of 1.9×10^6 g/m^3, Poisson's ratio in creep of 0.5, and a pyrocarbon creep coefficient of 1.36×10^{-29} (MPa-n/m^2)$^{-1}$. These parametric values are not necessarily expected values, but were used here for purposes of benchmarking the statistical method. These parametric values were selected for this analysis to be consistent with what was used in the development of the Design Expert algorithm.

It was assumed in these analyses that the IPyC layer failed in all particles. Therefore, the stresses in the SiC layer in all cases were calculated assuming a cracked IPyC. In the new statistical approach, SiC stresses were computed initially according to Eq. (8), which meant that a set of correlation functions h_i was developed based on the nominal values of Table 2. In the Design Expert approach, SiC stresses for the cracked particles were computed directly from the algorithm described in Section 3.2. In both cases, the SiC layers in the cracked particles were evaluated for failure using Weibull statistics, assuming a mean strength of 1250 MPa and a modulus of 6. Failure of the SiC layer was considered to constitute failure of the particle.

Failure probabilities obtained from these methods are compared in Table 3 for two hypothetical cases, where the six parameters were assumed to have Gaussian statistical distributions with standard deviations as shown in the table. The two cases are identical except for the magnitude of the standard deviations. The failure probabilities obtained from the two methods are equal for case 1 and are in close agreement for the larger standard deviations of case 2. The larger standard deviations in this case resulted in a lower failure probability. These verification analyses indicate that the use of Eq. (8) produces a very accurate estimate of the failure probability (assuming accuracy of the input to the analysis).

The results of Table 3 demonstrate a close correlation between Eq. (8) and the Design Expert algorithm when both are developed from the same set of mean values for the parameters. This indicates that Eq. (8), which is much easier to develop than a Design Expert algorithm, can be used as a standard for measuring accuracy of the simplified equation, Eq. (9). The Eq. (8) must, however, be developed from a set of mean parametric values representing the batch of particles under consideration. The results of benchmark calculations for Eq. (9) are presented below.

6.2. New method without correlation functions

Benchmark calculations were performed to evaluate accuracy of the new method when Eq. (9) is used to calculate the SiC stresses. It is anticipated that Eq. (9) will typically be used (possibly modified as discussed in Section 7) to determine batch failure probabilities, since it does not require developing correlation functions for all parameters. Eq. (9) was used to calculate failure probabilities for the four cases shown in Table 4, which again involved statistical variations in the six parameters of Table 2. The standard deviations in all cases were set equal to those of case 1 in Table 3. The mean values for case 1 equal those of case 1 in Table 3, which also match the nominal values of Table 2. To test Eq. (9) for other conditions, the mean values selected for cases 2 and 3 differ measurably from these nominal values. All of the mean values in case 4 were set to outer limits of the parametric ranges shown in Table 2.

Because the verification analyses of Table 3 demonstrate a high level of accuracy in the use of Eq. (8), this was used as a standard for measuring accuracy of Eq. (9). Therefore, results obtained from Eq. (9) for the four cases of Table 4 were compared to results obtained from Eq. (8) for the same cases. Results from Eq. (8) for the first case come directly from Table 3. Using Eq. (8) for the other three cases required that a new set of

Table 3
Comparison of failure probability calculations for two statistical methods

Case	Mean values and standard deviations						% Failed	
	IPyC thickness (μm) (SD)	SiC thickness (μm) (SD)	OPyC thickness (μm) (SD)	IPyC density (10^6 g/m^2) (SD)	IPyC BAF (SD)	Irradiation temperature (°C) (SD)	Design Expert	New method, Eq. (8)
1	40 (5)	35 (5)	43 (5)	1.90 (0.02)	1.16 (0.02)	1000 (30)	0.83	0.83
2	40 (6)	35 (5)	43 (6)	1.90 (0.05)	1.16 (0.04)	1000 (50)	0.69	0.72

Table 4
Comparison of failure probability calculations for new method, with and without the use of correlation functions

Case	Mean values						% Failed	
	IPyC thickness (μm)	SiC thickness (μm)	OPyC thickness (μm)	IPyC density (10^6 g/m^2)	IPyC BAF	Irradiation temperature (°C)	w/*h* functions (Eq. (8))	wo/*h* functions (Eq. (9))
1	40	35	43	1.90	1.16	1000	0.83	1.11
2	45	30	40	2.00	1.10	700	13.9	14.7
3	35	40	50	1.82	1.24	900	0.67	0.83
4	30	45	53	1.80	1.32	600	1.54	1.64

correlation functions h be developed for each case. The Design Expert algorithm was not used for verifying the new cases (2 through 4) because its regression analyses were centered on the nominal values of Table 2 rather than the mean values for the particle batches. Results in all four cases show that the use of Eq. (9) produced reasonable estimates for the failure probabilities. Improving the accuracy of Eq. (9) by including selected h functions from Eq. (8) is discussed in Section 7.

6.3. Eleven-parameter cases

To further test the use of Eq. (9) to estimate SiC stresses, two cases (shown in Table 5) were considered where the number of parameters that vary statistically about a mean value was increased from six to eleven. The mean values for case 1 match the nominal values from Table 1, while the mean values for case 2 differ significantly from these nominals. Creep amplification in these cases is simply a factor that is applied to creep values obtained from [11]. The Poisson's ratio in creep was set to 0.5 in both cases. Results from Eq. (9) were again compared to results obtained from Eq. (8), which required that a set of correlation functions h_i be developed for each of the two cases. Table 6 again shows reasonable agreement in results for these eleven-parameter cases.

Table 5
Statistical variations for eleven-parameter cases

Parameter	Mean value		Standard deviation	
	Case 1	Case 2	Case 1	Case 2
IPyC thickness (μm)	50	40	5	5
SiC thickness (μm)	25	35	3	5
OPyC thickness (μm)	50	40	5	5
IPyC density (10^6 g/m^3)	1.8	1.9	0.02	0.02
OPyC density (10^6 g/m^3)	1.8	1.9	0.02	0.02
IPyC BAF	1.24	1.06	0.02	0.015
OPyC BAF	1.04	1.06	0.01	0.015
Irradiation temperature (°C)	700	1000	30	30
Creep amplification	3	2	0.2	0.2
Kernel diameter (μm)	200	500	20	20
Buffer thickness (μm)	120	100	10	10

Table 6
Results for the eleven-parameter cases

Case	% Failed	
	Eq. (8)	Eq. (9)
1	0.75	0.64
2	0.0105	0.0065

It is noted that in the case where the standard deviations for all parameters are zero, then the stresses for the cracked particle in Eqs. (8) and (9) correctly reduce to $\sigma_{c\bar{v}}$. If the IPyC layer fails in all such particles, then the only variation considered among particles in a batch is the Weibull variation in strengths for the SiC layer. The failure probability in this situation is in principle given exactly by Eq. (14). Since Eqs. (8) and (9) reduce to $\sigma_{c\bar{v}}$ and the PARFUME Code performs Weibull statistics according to Eq. (14), both equations produce the correct failure probability for this case. Because Eq. (9) correctly reduces to $\sigma_{c\bar{v}}$ when there are no statistical variations in the parameters, it will at a minimum capture the failures associated with the Weibull distribution in SiC strength. Therefore, it should in any case capture these failures and at least a portion of those associated with statistical variations in the parameters. The accuracy in any particular situation depends, of course, on validity of the input to the analysis.

7. Improving the accuracy of Eq. (9)

The benchmark calculations of Section 6 show that predictions using Eq. (9) are in reasonable agreement with those obtained from Eq. (8). If desired, though, it is possible to improve the accuracy of Eq. (9) by including selected h functions from Eq. (8). To aid in the selection of parameters for this purpose, Table 7 lists the range of values for the function h (over a span of ± 4 standard deviations) for each of the parameters of cases 1 and 2

Table 7
Range in values for h functions for eleven-parameter cases

Parameter	Case 1	Case 2
IPyC thickness	0.71–1.09	0.59–1.33
SiC thickness	0.96–1.09	1.00–1.19
OPyC thickness	0.83–1.27	0.68–1.63
IPyC density	0.99–1.05	0.99–1.10
OPyC density	0.97–1.00	0.97–1.02
IPyC BAF	0.96–1.03	0.89–1.16
OPyC BAF	0.96–1.04	0.87–1.17
Irradiation temperature	1.00–1.06	0.91–1.06
Creep amplification	1.00–1.00	0.97–1.02
Kernel diameter	0.98–1.02	0.99–1.04
Buffer thickness	0.98–1.01	0.93–1.11

from Table 5. These ranges would be affected by a change in the magnitude of the standard deviations. In both cases, though, the functions for the IPyC, SiC, and OPyC thicknesses have smaller minimums or larger maximums than those of the other parameters. In case 2, the maximums for the IPyC and OPyC BAF are close to that of the SiC thickness, but the maximums for these functions are more equally balanced by their minimums. This suggests that including h functions for the three layer thicknesses would have the greatest effect in improving accuracy of Eq. (9). This was done for the two cases from Table 5 and the four cases from Table 4, with results shown in Table 8. In all cases, the results are quite close to those from Eq. (8). Including h functions for three parameters requires performing six additional ABAQUS runs to determine the failure probability for a particle batch, which is manageable. The analyst has the option to add as many functions to Eq. (9) as desired using Table 7 as a guide.

Table 8
Results for improved Eq. (9)

Case	% Failed	
	Eq. (8)	Eq. (9) improved
1, Table 5	0.75	0.73
2, Table 5	0.0105	0.0115
1, Table 4	0.83	0.91
2, Table 4	13.9	14.1
3, Table 4	0.67	0.72
4, Table 4	1.54	1.62

It is expected that larger standard deviations in the parameters will diminish the accuracy of results obtained from the use of Eqs. (8) or (9). In a practical sense, though, the standard deviations for an actual particle batch should not be appreciably larger than those of Table 5, since values in Table 5 envelop what has been observed in actual production runs for coated fuel particle.

Results above indicate that Eq. (9) can typically be used to produce reasonable estimates for failure probabilities in a general batch of fuel particles. The accuracy of these estimates can be improved by including selected h functions of Eq. (8) or by using Eq. (8) in its entirety. This approach, as summarized in Fig. 8, will treat statistical variations in all of the design parameters for TRISO-coated fuel particles. It is described above in terms of fuel particles having a cracked IPyC, but should also be applicable to other multi-dimensional behavior. Therefore, this method should facilitate the development of a fuel performance code that is capable of treating multi-dimensional failure mechanisms together with statistical variations in a wide range of design parameters.

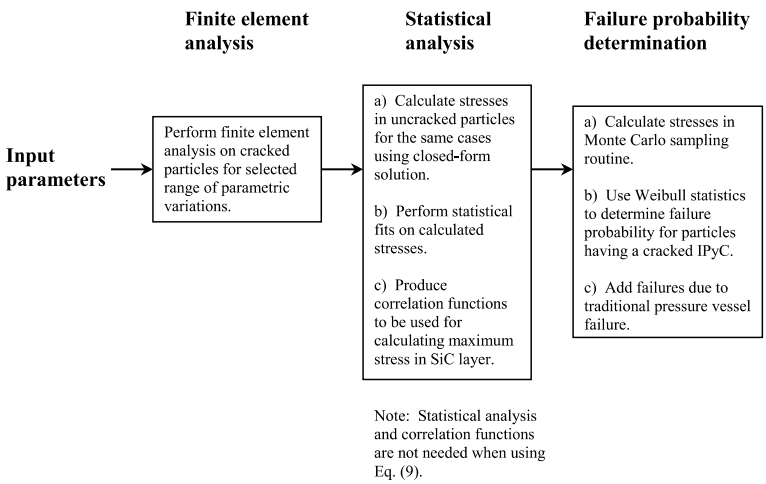

Fig. 8. Flow diagram for general statistical approach.

8. Application to NP-MHTGR experiments

The current version of the PARFUME code, which employs the statistical approach described above, has been used to analyze three irradiation experiments conducted as part of the NP-MHTGR program in the early 1990s. Fuel compacts were irradiated at the High Flux Isotope Reactor and the Advanced Test Reactor in the United States. TRISO-coated particles containing high-enriched uranium were irradiated at temperatures between 750 and 1250 °C, burnups between 65% and 80% FIMA, and fluences between 2 and 3.8×10^{25} n/m^2. On-line fission gas release measurements indicated significant failures during irradiation. PIE of individual fuel compacts revealed the presence of radial cracks in all layers of the TRISO coating. The irradiation conditions for the experiments are summarized in Table 9, while the levels of cracking measured during PIE are shown in Table 10. The particle dimensions, burnup, end-of-life fluence, irradiation temperature, ^{235}U enrichment, densities and BAF for the pyrocarbons, etc., were based on fabrication records for the fuel and on the service conditions measured during irradiation for each experiment.

To assess the effect of temperature variability during irradiation on particle stresses, ABAQUS calculations were performed with both the actual volume averaged temperature history and the time averaged volume averaged temperature for NPR-1 compact A5. The actual volume averaged temperature for the compact varied from about 1150–870 °C during the experiment, while the time averaged, compact volume averaged temperature was 987 °C [17]. Calculated time histories for principal stresses in the SiC layer are presented in Fig. 9, which show that the stress histories compare closely for these two cases. These results indicate that using a time averaged volume averaged temperature in the PARFUME predictions is a good approximation to the use of actual temperature histories.

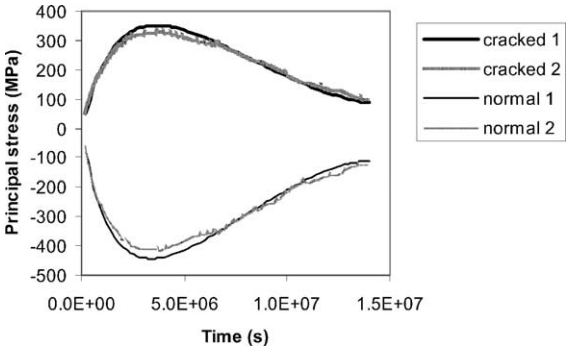

Fig. 9. SiC stress history comparisons for (1) time averaged temperature vs. (2) actual temperature in cracked and uncracked particles of NPR-1 A5 irradiation experiment.

Weibull parameters for the IPyC and SiC were very similar to those used in the benchmark calculations of Section 6. Included in the results shown in Table 10 (column 5) are the percentage of particles predicted to have a cracked IPyC and the percentage of particles predicted to fail because of a cracked SiC. Because the PIE indicated that the OPyC failed in almost all cases, evidently as a result of the presence of a protective outer pyrocarbon layer in these particles, the OPyC layer was removed in these analyses. The calculations did not account for stress concentrations in the SiC that may have

Table 9
Irradiation conditions for NPR experiments

Fuel compact ID	Fast fluence (10^{25} n/m^2)	Irradiation temperature (°C), average	Burnup (% FIMA)
NPR-2 A4	3.8	746	79
NPR-1 A5	3.8	987	79
NPR-1 A8	2.4	845	72
NPR-1A A9	1.9	1052	64

Table 10
Comparisons of ceramographic observations to PARFUME calculations for TRISO coated fissile fuel particles

Fuel compact ID	Sample size	% Failed	95% Confidence interval (%)	Calculated	Calculated with $1.8 \times$ creep
IPyC Layer[a]					
NPR-2 A4	83	65	$54 < p < 76$	100	99.8
NPR-1 A5	39	31	$17 < p < 47$	100	34.8
NPR-1 A8	53	6	$2 < p < 16$	100	94.0
NPR-1A A9	17	18	$5 < p < 42$	100	14.5
SiC Layer[a]					
NPR-2 A4	287	3	$2 < p < 6$	9.2	3.4
NPR-1 A5	178	0.6	$0 < p < 3$	1.8	0.22
NPR-1 A8	260	0	$0 < p < 2$	5.9	1.8
NPR-1A A9	83	1	$0 < p < 5$	1.1	0.044

[a] Layer failure is considered to be a through wall crack as measured by PIE.

resulted from OPyC cracking. It is seen that PARFUME predicts that the IPyC layer cracks in 100% of the particles for every compact tested. As shown in the table, the PIE revealed that the actual failure fractions were less than this. Based on historical literature sources, it is believed that the creep coefficients recommended in [11] and currently used in the PARFUME code may be too low, which would allow the calculated shrinkage stresses to reach too high a value before creep relaxation takes effect. If the creep coefficients used in the analyses were amplified by a factor of 1.8, which is closer to values used in older performance models [18,19], the number of failures in the IPyC and SiC decrease as shown in Table 10 (column 6). The higher creep gives better agreement with the experimental results.

Eq. (9) was used to calculate the failure probabilities in Table 10. It should give reasonable accuracy since the standard deviations for the IPyC and SiC thicknesses were less than 4 μm, and the OPyC layer was assumed to be ineffective. Standard deviations for other parameters were such that including correlation, h, functions for them would have very little effect. It is noted that because the ratio $\sigma_{c\bar{v}}/\sigma_{u\bar{v}}$ maintained essentially the same value for all four NPR compacts (~0.67), only one finite element analysis of a cracked particle would have been needed to generate the failure probabilities of Table 10.

9. Implications on fuel design

The results from our fuel performance model, though not fully validated, have preliminary implications on coated particle fuel design. Our modeling indicates that the development of cracks in the IPyC layer results in tensile stresses in the SiC layer high enough to cause failure. Cracking of the IPyC is the result of excessive anisotropy in the layer. The excessive anisotropy has been attributed to active gas coating concentrations in the chemical vapor deposition coater that result in deposition of the layer at too low a rate [20]. IPyC coated at low coating rates (~1 to 4 μm/min) is known to have unacceptable anisotropy and under irradiation will fail. Our studies on trying to minimize this effect suggests that the tensile stress in the SiC near the IPyC crack scales with the thickness of the IPyC layer. As the thickness of the cracked IPyC layer increases, the tensile stress in the SiC increases. Based on our modeling to date and the results of the NP-MHTGR irradiations, it does not appear that acceptable irradiation and high temperature accident test performance can be achieved with coated particle fuel in which a crack exists in the IPyC layer. A simple and practical solution to avoiding cracking of the IPyC layer and the subsequent threat to particle integrity is to fabricate it at coating rates (>4 μm/min) that result in more isotropic pyrocarbon [20].

10. Conclusions

The INEEL is in the process of developing an integrated mechanistic fuel performance model for TRISO-coated gas reactor particle fuel named PARFUME, with the objective of physically describing the behavior of the fuel particle under irradiation. As part of this effort, a method has been developed for efficiently estimating stresses in the SiC layer of fuel particles that have a cracked IPyC layer. When the effect of shrinkage cracks are included, predictions for failure probabilities are in reasonable agreement with those observed in the NP-MHTGR fuel irradiation experiments. It is intended that other relevant multi-dimensional effects, such as partial debonding between coating layers and asphericity, will also be included in the model.

PARFUME will also model the physico-chemical behavior of coated particle fuel to address the following phenomena:

- fission product gas release from the kernel and CO/CO_2 production as a function of burnup, temperature and kernel type (oxide, carbide, oxycarbide);
- fission product inventory as a function of burnup and enrichment of the particle;
- chemical changes of the fuel kernel during irradiation (changes in carbon/oxygen, carbon/metal and/or oxygen/metal ratio depending on the kernel type) and its influence on fission product and/or kernel attack on the particle coatings;
- kernel migration;
- fission product diffusion, migration, and segregation.

Acknowledgements

This work was performed for the US Department of Energy Office of Nuclear Energy under DOE Idaho Operations Office contract DE-AC07-99ID13727. The authors appreciate a review of the article provided by Abderrafi Ougouag of the Idaho National Engineering and Environmental Laboratory.

References

[1] J.L. Kaae, J. Nucl. Mater. 32 (1969) 322.
[2] D.W. Stevens, Nucl. Tech. 10 (1971) 301.
[3] T.D. Gulden et al., Nucl. Tech. 16 (1972) 100.
[4] K. Bongartz, Nucl. Tech. 35 (1977) 379.
[5] H. Walther, Nucl. Eng. Design 18 (1971) 11.
[6] K. Bongartz, Status of the Fuel Stress and Failure Rate Calculations at KFA, JÜL-1686, KFA Jülich, GmbH, 1980.
[7] G.K. Miller, R.G. Bennett, J. Nucl. Mater. 206 (1993) 35.
[8] D.G. Martin, Nucl. Eng. Design 213 (2002) 241.
[9] G.K. Miller, D.A. Petti, D.J. Varacalle, J.T. Maki, J. Nucl. Mater. 296 (2001) 205.

[10] ABAQUS User's Manual, Version 5.8, Hibbitt, Karlsson, and Sorenson, Inc., 1998.
[11] NP-MHTGR Material Models of Pyrocarbon and Pyrolytic Silicon Carbide, CEGA Corporation, CEGA-002820, Rev. 1, 1993.
[12] P. Whitcomb et al., Design-Expert, Version 4.0, Stat-Ease, 1993.
[13] G.E.P. Box, W.G. Hunter, J.S. Hunter, Statistics for Experimenters, Wiley, England, 1978.
[14] G.K. Miller, D.C. Wadsworth, J. Nucl. Mater. 211 (1994) 57.
[15] N.N. Nemeth, J.M. Mandershield, J.P. Gyekenyesi, Ceramics Analysis and Reliability Evaluation of Structures (CARES) User's and Programmer's Manual, NASA Technical Paper 2916, 1989.
[16] A.E. Green, A.J. Bourne, Reliability Technology, John Wiley and Sons, New York, 1972, p. 244.
[17] C.A. Baldwin et al., The New Production Reactor Fuel Post Irradiation Examination Data Report for Capsules NPR 1, NPR 2, and NPR 1A, Oak Ridge National Laboratory Report ORNL/M-2849, 1993.
[18] J. Kaae, D. Stevens, C. Luby, Nucl. Tech. 10 (1971) 44.
[19] D.G. Martin, Physical and Mechanical Properties of the Constituents of Coated Fuel Particles and the Effect of Irradiation, HTR-F WP3 Meeting, Lyon, 2001.
[20] D.A. Petti et al., Key Differences in the Fabrication, Irradiation and Safety Testing of US and German TRISO-coated Particle Fuel and Their Implications on Fuel Performance, Idaho National Engineering and Environmental Laboratory Report INEEL/EXT-02-0300, 2002.